

Exploring The Potential Of GANs In Biological Sequence Analysis

Taslim Murad, Sarwan Ali and Murray Patterson

Department of Computer Science, Georgia State University, Atlanta, USA

{tmurad2,sali85}@student.gsu.edu, mpatterson30@gsu.edu

Abstract—Biological sequence analysis is an essential step toward building a deeper understanding of the underlying functions, structures, and behaviors of the sequences. It can help in identifying the characteristics of the associated organisms, like viruses, etc., and building prevention mechanisms to eradicate their spread and impact, as viruses are known to cause epidemics which can become pandemics globally. New tools for biological sequence analysis are provided by machine learning (ML) technologies to effectively analyze the functions and structures of the sequences. However, these ML-based methods undergo challenges with data imbalance, generally associated with biological sequence datasets, which hinders their performance. Although various strategies are present to address this issue, like the SMOTE algorithm, which create synthetic data, however, they focus on local information rather than the overall class distribution. In this work, we explore a novel approach to handle the data imbalance issue based on Generative Adversarial Networks (GANs) which use the overall data distribution. GANs are utilized to generate synthetic data that closely resembles the real one, thus this generated data can be employed to enhance the ML models' performance by eradicating the class imbalance problem for biological sequence analysis. We perform 3 distinct classification tasks by using 3 different sequence datasets (Influenza A Virus, PALMdb, VDjDB) and our results illustrate that GANs can improve the overall classification performance.

Index Terms—Sequence Classification, GANs, Bio-sequence Analysis, Class Imbalance.

I. INTRODUCTION

Biological sequences usually refer to nucleotides or amino acids-based sequences and their analysis can provide detailed information about the functional and structural behaviors of the corresponding viruses which are usually responsible for causing diseases, for example, Flu [1], Covid-19 [2], etc. This information is very useful in building prevention mechanisms, like drugs [3], vaccines [4], etc., and to control the disease spread, eliminate the negative impacts, and do virus spread surveillance.

Influenza A Virus (IAV) is such an example, which is responsible for causing a highly contagious respiratory illness that can significantly threaten global public health. As the Centers for Disease Control and Prevention Center (CDC) ¹ reports that so far this season, there have been at least 25 million illnesses, 280,000 hospitalizations, and 17,000 deaths from Flu in the United States. Therefore, identifying and tracking the evolution of IAV accurately is a vital step in the fight against this virus. Classification of IAV is an essential

task in this aspect as it can provide valuable information on the origin, evolution, and spread of the virus. Moreover, the identification of the viral taxonomy can further enrich its understanding, like the viral polymerase palmprint sequence of a virus is utilized to determine its taxonomy (species generally) [5]. A polymerase palmprint is a unique sequence of amino acids located at the thumb subunit of the viral RNA-dependent polymerase. Furthermore, examining the antigen specificities based on the T-cell receptor sequences can provide beneficial information regarding solving numerous problems of both basic and applied immunology research.

Many traditional sequence analysis methods follow phylogeny-based techniques [6], [7] to identify sequence homology and predict disease transmission. However, the availability of large-size sequence data exceeds the computational limit of such techniques.

Moreover, the application of ML approaches for performing biological sequence analysis is a popular research topic these days [8], [9]. The ability of ML methods to determine the sequence's biological functions makes them desirable to be employed for sequence analysis. Additionally, ML models can also determine the relationship between the primary structure of the sequence and its biological functions. Like [8] built a Random Forest-based algorithm to classify sucrose transporter (SUT) protein, [9] designed a novel tool for Protein-protein interactions data and functional analysis, [10] developed a new ML model to identify RNA pseudo-uridine modification sites. ML-based biological sequence analysis approaches can be categorized into feature-engineering-based methods [11], [12], kernel-based methods [13], neural network-based techniques [14], [15], and pre-trained deep learning models [16], [17]. However, extrinsic factors limit the performance of ML-based techniques and one such major factor is data imbalance, as in the case of biological sequences the data is generally imbalanced because the number of negative samples is much larger than that of positive samples [18]. ML models can obtain the best results when the dataset is balanced while unbalanced data will greatly affect the training of machine learning models and their application in real-world scenarios [19].

In this paper, we explore the idea to improve the performance of ML methods for biological sequence analysis by eradicating the data imbalance challenge using Generative Adversarial Networks (GANs). Our method leverages the strengths of GANs to effectively analyze these sequences,

¹<https://www.cdc.gov/flu/weekly/index.htm>

with the potential to have significant implications for virus surveillance and tracking, as well as the development of new antiviral strategies.

Our contributions to this work are as follows:

- 1) We explore the idea to do biological sequence classification using Generative Adversarial Networks (GANs).
- 2) We show that usage of GANs improves predictive performance by eliminating the data imbalance challenge.
- 3) We demonstrated the potential implications of the proposed approach for virus surveillance and tracking, and for the development of new antiviral strategies.

The rest of the paper is organized as follows: Section II contains the related work. The proposed approach details are enlisted in Section III. The datasets used in the experiments along with the ML models and evaluation metrics information is provided in Section IV. Section V highlights the experimental results and their discussion. Finally, the paper is concluded in Section VI.

II. RELATED WORK

The combination of biological sequence analysis and ML models has gained quite a lot of attention among researchers in recent years [8], [9]. As a biological sequence consists of a long string of characters corresponding to either nucleotides or amino acids, it needs to be transformed into a numerical form to make it compatible with the ML model. Various numerical embedding generation mechanisms are proposed to extract features from the biological sequences [11], [14], [17].

Some of the popular embedding generation techniques use the underlying concept of k -mer to compute the embeddings. Like [20] uses the k -mers frequencies to get the vectors, [12], [21] combine position distribution information and k -mers frequencies for getting the embeddings. Other approaches [14], [15] are employing neural networks to obtain the feature vectors. Moreover, kernel-based methods [13] and pre-trained deep learning models-based methods [16], [17] also play a vital role in generating the embeddings. Although all these techniques illustrate promising analysis results, however, they haven't mentioned anything about dealing with data imbalance issues, which if handled properly will yield performance improvement.

Furthermore, another set of methods tackles the class imbalance challenge with the aim to enhance overall analytical performance. They use resampling techniques at the data level by either oversampling the minority class or undersampling the majority class. For instance, [8] uses Borderline-SMOTE algorithm [22], an oversampling approach, to balance the feature set of the sucrose transporter (SUT) protein dataset. However, as Borderline-SMOTE is based on the k nearest neighbor algorithm so it has high time complexity, is susceptible to noise data, and cannot make good use of the information of the majority samples [23]. Similarly, [24] does protein classification by handling the data imbalance using a hybrid sampling algorithm that combines both ensemble classifier and over-sampling techniques, KernelADASYN [25] employs a kernel-based adaptive synthetic over-sampling approach to

deal with data imbalance. However, these methods don't utilize the overall data distribution, rather only are based on local information [26].

III. PROPOSED APPROACH

In this section, we will discuss our idea of exploring GANs to obtain analytical performance improvement for biological sequences in detail. As our input sequence data consists of string sequences representing amino acids, they need to be transformed into numerical representations in order to operate GANs on them. For that purpose, we use 4 distinct and effective numerical feature generation methods which are described below.

A. Spike2Vec [20]

Spike2Vec generates the feature embedding by computing the k -mers of a sequence. As k -mers are known to preserve the ordering information of the sequence. K -mers represent a set of consecutive substrings of length k driven from a sequence. For s sequence with length N , the total number of its k -mers will be $N - k + 1$. This method devises the feature vector for a sequence by capturing the frequencies of its k -mers. To further deal with the curse of dimensionality issue, Spike2Vec uses random Fourier features (RFF) to map data to a randomized low-dimensional feature space. We use $k = 3$ to get the embeddings.

B. PWM2Vec [21]

This method works by using the concept of k -mers to get the numerical form of the biological sequences, however, rather than utilizing constant frequency values of the k -mers, it assigns weights to each amino acid of the k -mers and employs these weights to generate the embeddings. The position weight matrix (PWM) is used to determine the weights. PWM2Vec considers the relative importance of amino acids along with preserving the ordering information. The workflow of this method is illustrated in Figure 1. Our experiments use $k = 3$ to obtain the embeddings.

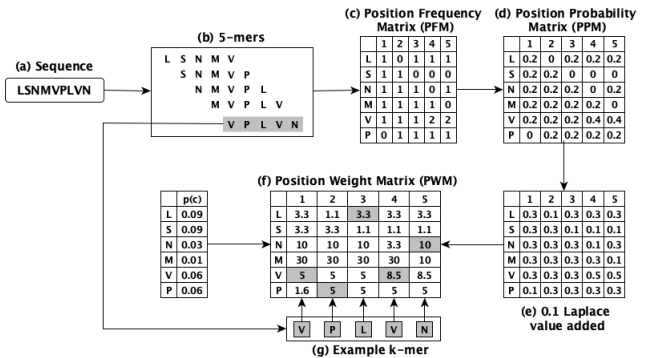


Fig. 1: The workflow of PWM2Vec method for a given sequence.

C. Minimizer

This approach is based on the utility of minimizers [27] (m -mer) to get the feature vectors of sequences. The minimizer is extracted from a k -mer and it is a m length lexicographically smallest (in both forward and backward order) substring of consecutive alphabets from the k -mer. Note that $m < k$. The workflow of computing minimizers for a given input sequence is shown in Figure 2. This approach intends to eliminate the redundancy issue associated with k -mers, hence improving the storage and computation cost. Our experiments used $k = 9$ and $m = 3$ to generate the embeddings.

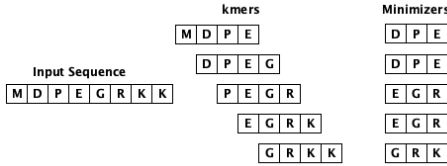


Fig. 2: The workflow of getting minimizers from an input sequence.

After getting the numerical embeddings of the biological sequences using the methods mentioned above, we further utilize these embeddings to train our GAN model. This model has two parts, a generator model and a discriminator model. Each discriminator and generator model consists of two inner dense layers with ReLU activation functions (each followed by a batch-normalization layer) and a final dense layer. In the discriminator, the final dense layer has a Sigmoid activation function while the generator has a Softmax activation function. The generator's output has dimensions the same as the input data, as it synthesizes the data, while the discriminator yields a binary scalar value to indicate if the generated data is fake or real.

The GAN model is trained using cross-entropy loss function, ADAM optimizer, 32 batch size, and 1000 iterations. The steps followed to obtain the synthetic data after the training GAN model is illustrated in the Algorithm 1. As given in the algorithm, firstly generator and discriminator models are created in steps 1-2. Then the discriminator model is compiled for training with cross-entropy loss and ADAM optimizer in step 3. After that, the count and length of synthetic sequences along with the number of training epochs and batch size are mentioned in steps 4-6. Then the training of the models is happening in 7-12 steps, where each of the models is fine-tuned for the given number of iterations. Once the GAN model is trained, its generator part is employed to synthesize new embedding data which resembles real-world data. This synthesized data can eliminate the data imbalance problem, improving the analytical performance. Moreover, the workflow of GAN is shown in Figure 3.

IV. EXPERIMENTAL SETUP

This section highlights the details of the datasets used to conduct the experiments along with the information about the

Algorithm 1 GAN Model.

Input: Set of Sequences S , $ganCnt$
Output: GANs based sequences S'

- 1: $m_gen \leftarrow generator()$ ▷ generator model
- 2: $m_dis \leftarrow discriminator()$ ▷ discriminator model
- 3: $m_dis.compile(loss = CE, opt = ADAM)$
- 4: $seqLen \leftarrow len(S[0])$ ▷ len of each S' sequence
- 5: $iter \leftarrow 1000$
- 6: $batch_size \leftarrow 32$
- 7: **for** i **in** $iter$ **do**
- 8: $noise \leftarrow RANDOM(ganCnt, seqLen)$
- 9: $S' \leftarrow m_gen.predict(noise)$ ▷ get GAN sequences
- 10: $m_dis.backward(m_dis.loss)$ ▷ fine-tune m_dis
- 11: $m_gen.backward(m_gen.loss)$ ▷ fine-tune m_gen
- 12: **end for**
- 13: **return**(S')

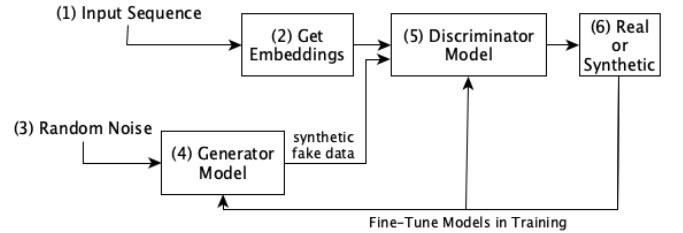


Fig. 3: The workflow of the GAN model.

classification models and their respective evaluation metrics to report the performance. All experiments are carried out on Intel (R) Core i5 system with a 2.40 GHz processor and 32 GB memory.

A. Dataset Statistics

We use 3 different datasets to evaluate our suggested method. A detailed description of each of the dataset is given as follow,

1) *Influenza A Virus*: We are using the influenza A virus sequence dataset belonging to two kinds of subtypes "H1N1" and "H3N2" extracted from [28] website. This data contains 222,450 sequences in total with 119,100 sequences belonging to the H1N1 subtype and 103,350 to the H2N3 subtype. The detailed statics for this dataset is shown in Table I. We use these two subtypes as labels to classify the Influenza A virus in our experiments.

2) *PALMdb*: The PALMdb [5], [29] dataset consists of viral polymerase palmprint sequences which can be classified species-wise. This dataset is created by mining the public sequence databases using the palmscan algorithm. It has 124,908 sequences corresponding to 18 different virus species. The distribution of these species is given in Table II and more detailed statistics are shown in Table I. We use the species name as a label to do the classification of the PALMdb sequences.

TABLE I: Dataset Statistics of each dataset used in our experiments.

Name	Sequences	Classes	Goal	Sequence Length		
				Min	Max	Average
Influenza A Virus	222450	2	Virus Subtypes Classification	11	71	68.60
PALMdb	124908	18	Virus Species Classification	53	150	130.83
VDjDB	78344	17	Antigen Species Classification	7	20	12.66

TABLE II: Species-wise distribution of PALMdb dataset.

Species Name	Count	Species Name	Count
Avian orthoavulavirus 1	2353	Chikungunya virus	2319
Dengue virus	1627	Hepacivirus C	29448
Human orthopneumovirus	3398	Influenza A virus	47362
Influenza B virus	8171	Lassa mammarenavirus	1435
Middle East respiratory syndrome-related coronavirus	1415	Porcine epidemic diarrhea virus	1411
Porcine reproductive and respiratory syndrome virus	2777	Potato virus Y	1287
Rabies lyssavirus	4252	Rotavirus A	4214
Turnip mosaic virus	1109	West Nile virus	5452
Zaire ebolavirus	4821	Zika virus	2057

3) *VDjDB*: *VDjDB* is a curated dataset of T-cell receptor sequences with known antigen specificities [30]. This dataset consists of 58,795 human TCRs and 3,353 mouse TCRs. More than half of the examples are TRBs ($n=36,462$) with the remainder being TRAs ($n=25,686$). It has total 78,344 sequences belonging to 17 unique antigen species. The distribution of the sequence among the antigen species is shown in Table III and further details of the dataset are given in Table I. We use this data to perform the antigen species classification.

Our code and preprocessed datasets are available online for reproducibility ².

TABLE III: Antigen Species-wise distribution of *VDjDB* dataset.

Antigen Species Name	Count	Antigen Species Name	Count
CMV	37357	DENV1	180
DENV3/4	177	EBV	11026
HCV	840	HIV-1	3231
HSV-2	154	HTLV-1	232
HomoSapiens	4646	InfluenzaA	14863
LCMV	141	MCMV	1463
PlasmodiumBerghei	243	RSV	125
SARS-CoV-2	758	SIV	2119
YFV	789		

B. Data Visualization

We visualize our datasets using the popular visualization technique, t-SNE [31], to view the internal structure of each dataset following various embeddings. Like, the plots for the Influenza A Virus dataset are reported in Figure 4. We can observe that for Spike2Vec and Minimizer based plots, the addition of GANs-based features is causing two big clusters along with the small scattered clusters for each, unlike their original t-SNEs which only consist of small scattered groups.

²Available in the published version

However, the PWM2Vec-based plots for both with GANs and without GANs show similar structures. But generally including GANs-based embeddings to the original ones can improve the t-SNE structure.

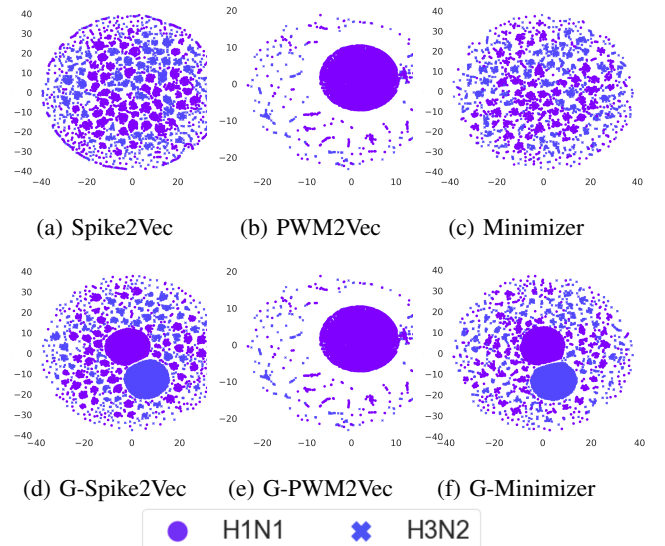


Fig. 4: t-SNE plots for Influenza A Virus dataset without GANs (a, b, c) and with GANs (d, e, f). The figure is best seen in color.

Moreover, the t-SNE plots for PALMdb dataset corresponding to different embeddings are shown in Figure 5. We can observe that this dataset shows similar kinds of cluster patterns corresponding to both without GANs and with GANs based embeddings. As the original dataset is already portraying clear distinct clusters for various species, therefore adding GANs-based embedding to it is not affecting the cluster structure much.

Furthermore, the t-SNE plots for *VDjDB* dataset are given in Figure 6. We can observe that the addition of GAN-based features to the Minimizer-based embedding has yielded more clear and distinct clusters in the visualization. GAN-based spike2vec also portrays more clusters than the Spike2Vec one. However, the PWM2Vec shows similar patterns for both GAN-based and without GANs embeddings. Overall, it indicates that adding GANs-based features is enhancing the t-SNE cluster structures.

We also investigated the t-SNE structures generated by using only the GANs-based embeddings and Figure 7 illustrates the results. It can be seen that for all the datasets only GAN embeddings are yielding non-overlapping distinct clusters corresponding to each group with respect to the dataset. It is because for each group the only-GAN embeddings are synthesized after training the GAN model with the original data of the respective group.

C. ML Classifiers and Evaluation Metrics

To perform classification tasks we employ the following ML models: Naive Bayes (NB), Multilayer Perceptron (MLP),

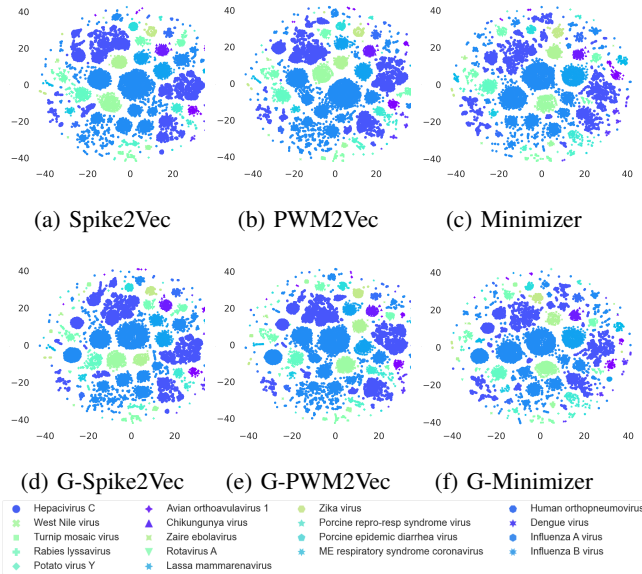


Fig. 5: t-SNE plots for PALMdb dataset without GANs (a, b, c), and with GANs (d, e, f). The figure is best seen in color.

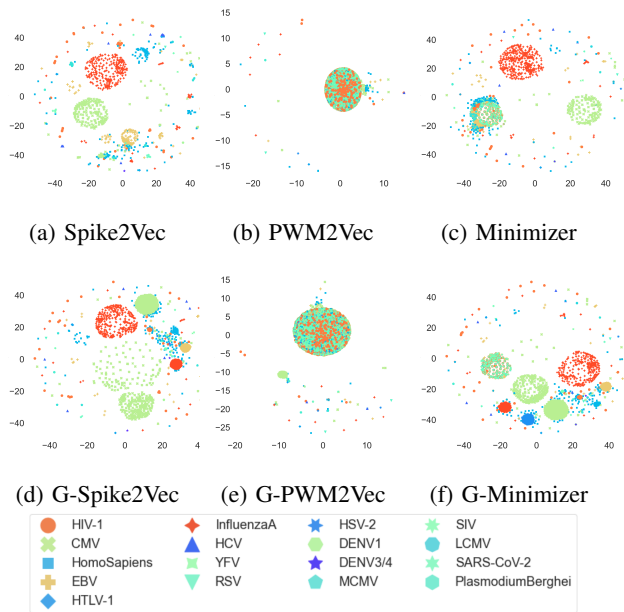


Fig. 6: t-SNE plots for VDjDB dataset without GANs (a, b, c) and with GANs (d, e, f). The figure is best seen in color.

k-Nearest Neighbor (k-NN) (where $k = 3$), Random Forest (RF), Logistic Regression (LR), and Decision Tree (DT). For each classification task, the data is split into 70-30% train-test sets using stratified sampling to preserve the original data distribution. Furthermore, our experiments are conducted by averaging the performance results of 5 runs for each combination of dataset and classifier to get more stable results.

We evaluated the classifiers using the following performance metrics: accuracy, precision, recall, weighted F1, F1

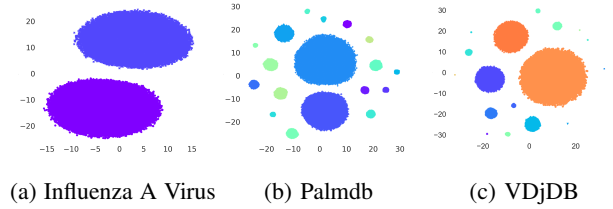


Fig. 7: t-SNE plots of only GANs embeddings for Influenza A Virus, PALMdb, and VDjDB datasets. The figure is best seen in color.

macro, and ROC AUC macro. Since we are doing multi-class classification in some cases, we utilized the one-vs-rest approach for computing the ROC AUC score for them. Moreover, the reason for reporting many metrics is to get more insight into the classifiers' performance, especially in the class imbalance scenario where reporting only accuracy does not provide sufficient performance information.

V. RESULTS AND DISCUSSION

This section discusses the experimental results comprehensively. The subtype classification results of the Influenza A virus dataset are given in Table IV, along with the results of the PALMdb dataset species-wise classification. The antigen species-wise classification results of VDjDB data are shown in Table V. The reported results represent the test set results. The further details are as follows,

A. Performance of Original Data

These results illustrate the classification performance achieved corresponding to the embeddings generated by Spike2Vec, PWM2Vec, and Minimizer strategies for each dataset. We can observe that for the Influenza A Virus dataset, Spike2Vec and Minimizer are exhibiting similar performance for almost all the classifiers and are better than PWM2Vec. However, the NB model yields minimum predictive performance for all the embeddings. Similarly, the VDjDB dataset portrays similar performance for Spike2Vec and Minimizer for all evaluation metrics, while its PWM2Vec has a very low predictive performance. Moreover, all the embeddings achieve the same performance in terms of all the evaluation metrics for every classifier on the PALMdb dataset.

B. Performance of Original Data with GANs

To view the impact of GAN-based data on the predictive performance for all the datasets, we evaluate the performance using the original embeddings with GAN-based synthetic data added to them respectively. This GANs-based data is used to train the classifiers, while only the original data is used as test data. To generate the GAN data corresponding to an embedding generation method, the GAN model is trained with the original embeddings first and then new data is synthesized for that embedding. Every label of the embedding will have a different count of synthetic data depending on its count in the

TABLE IV: The subtype classification results of Influenza A Virus dataset and species-wise classification results of PALmdb dataset. These results are average results over 5 runs.

Method	Influenza A Virus							PALmdb								
	Algo.	Acc. \uparrow	Prec. \uparrow	Recall \uparrow	F1 (Weig.) \uparrow	F1 (Macro) \uparrow	ROC AUC \uparrow	Train Time (Sec.) \downarrow	Acc. \uparrow	Prec. \uparrow	Recall \uparrow	F1 (Weig.) \uparrow	F1 (Macro) \uparrow	ROC AUC \uparrow	Train Time (Sec.) \downarrow	
Without GANs	Spike2Vec [20]	NB	0.538	0.673	0.538	0.382	0.358	0.503	96.851	0.999	0.999	0.999	0.999	0.999	0.999	453.961
		MLP	0.999	0.999	0.999	0.999	0.999	0.999	742.551	0.999	0.999	0.999	0.999	0.999	0.999	1446.421
		KNN	0.999	0.999	0.999	0.999	0.999	0.999	2689.320	0.999	0.999	0.999	0.999	0.999	0.999	1274.75
		RF	0.999	0.999	0.999	0.999	0.999	0.999	433.459	0.999	0.999	0.999	0.999	0.999	0.999	166.087
		LR	0.966	0.966	0.966	0.966	0.966	0.965	24.467	0.999	0.999	0.999	0.999	0.999	0.999	31564.898
		DT	0.999	0.999	0.999	0.999	0.999	0.999	54.024	0.999	0.999	0.999	0.999	0.999	0.999	163.827
	PWM2Vec [21]	NB	0.563	0.745	0.563	0.435	0.414	0.530	60.155	0.999	0.999	0.999	0.999	0.999	0.999	562.922
		MLP	0.644	0.785	0.644	0.579	0.566	0.617	1471.086	0.999	0.999	0.999	0.999	0.999	0.999	1675.896
		KNN	0.644	0.785	0.644	0.579	0.566	0.617	2665.538	0.999	0.999	0.999	0.998	0.999	0.999	1514.240
		RF	0.644	0.785	0.644	0.579	0.566	0.618	1514.979	0.999	0.999	0.999	0.999	0.999	0.999	284.450
		LR	0.644	0.784	0.644	0.579	0.565	0.617	388.235	0.999	0.999	0.999	0.999	0.999	0.999	41029.833
		DT	0.644	0.785	0.644	0.579	0.566	0.617	78.525	0.999	0.999	0.999	0.999	0.999	0.999	233.533
Minimizer	NB	0.679	0.682	0.679	0.673	0.669	0.670	57.469	0.999	0.999	0.999	0.999	0.999	0.999	474.482	
	MLP	0.998	0.998	0.998	0.998	0.998	0.998	1864.844	0.999	0.999	0.999	0.999	0.999	0.999	3958.188	
	KNN	0.999	0.999	0.999	0.999	0.999	0.999	2818.292	0.999	0.999	0.999	0.999	0.999	0.999	1357.673	
	RF	0.999	0.999	0.999	0.999	0.999	0.999	1039.824	0.999	0.999	0.999	0.999	0.999	0.999	399.507	
	LR	0.719	0.719	0.719	0.719	0.718	0.718	186.522	0.999	0.999	0.999	0.999	0.999	0.999	7270.111	
	DT	0.999	0.999	0.999	0.999	0.999	0.999	72.510	0.999	0.999	0.999	0.999	0.999	0.999	223.215	
With GANs	Spike2Vec [20]	NB	0.538	0.681	0.538	0.380	0.355	0.502	138.179	0.999	0.999	0.999	0.999	0.999	0.999	197.033
		MLP	0.992	0.992	0.992	0.992	0.992	0.992	1604.287	0.999	0.999	0.999	0.999	0.999	0.999	491.182
		KNN	0.999	0.999	0.999	0.999	0.999	0.999	3546.211	0.999	0.999	0.999	0.999	0.999	0.999	689.672
		RF	0.999	0.999	0.999	0.999	0.999	0.999	784.393	0.999	0.999	0.999	0.999	0.999	0.999	243.646
		LR	0.957	0.957	0.957	0.957	0.957	0.957	6810.398	0.999	0.999	0.999	0.999	0.999	0.999	2643.646
		DT	0.999	0.999	0.999	0.999	0.999	0.999	365.332	0.999	0.999	0.999	0.999	0.999	0.999	396.362
	PWM2Vec [21]	NB	0.565	0.748	0.565	0.437	0.416	0.532	107.617	0.999	0.999	0.999	0.999	0.999	0.999	569.510
		MLP	0.644	0.784	0.644	0.579	0.566	0.617	1817.859	0.999	0.999	0.999	0.999	0.999	0.999	1337.920
		KNN	0.646	0.785	0.646	0.581	0.568	0.619	2965.701	0.999	0.999	0.999	0.999	0.999	0.999	1524.009
		RF	0.646	0.786	0.646	0.582	0.569	0.619	1837.425	0.999	0.999	0.999	0.999	0.999	0.999	1802.577
		LR	0.632	0.793	0.632	0.589	0.597	0.657	10273.672	0.999	0.999	0.999	0.999	0.999	0.999	3549.095
		DT	0.646	0.786	0.646	0.581	0.568	0.619	1264.188	0.999	0.999	0.999	0.999	0.999	0.999	2580.831
Minimizer	NB	0.611	0.726	0.611	0.534	0.520	0.584	127.058	0.999	0.999	0.999	0.999	0.999	0.999	669.513	
	MLP	0.976	0.976	0.976	0.976	0.976	0.976	825.868	0.999	0.999	0.999	0.999	0.999	0.999	1231.650	
	KNN	0.999	0.999	0.999	0.999	0.999	0.999	3163.325	0.999	0.999	0.999	0.999	0.999	0.999	1484.555	
	RF	0.999	0.999	0.999	0.999	0.999	0.999	1557.065	0.999	0.999	0.999	0.999	0.999	0.999	1699.503	
	LR	0.711	0.712	0.711	0.711	0.710	0.711	2179.485	0.999	0.999	0.999	0.999	0.999	0.999	3482.345	
	DT	0.999	0.999	0.999	0.999	0.999	0.999	481.232	0.999	0.999	0.999	0.999	0.999	0.999	2700.860	
Only GANs For Training	Spike2Vec [20]	NB	0.443	0.318	0.443	0.296	0.317	0.476	69.293	0.056	0.005	0.056	0.009	0.014	0.523	172.517
		MLP	0.499	0.506	0.499	0.498	0.499	0.503	279.364	0.104	0.260	0.104	0.148	0.039	0.486	264.306
		KNN	0.586	0.623	0.586	0.523	0.510	0.561	4088.144	0.126	0.242	0.126	0.156	0.123	0.533	263.101
		RF	0.464	0.215	0.464	0.294	0.317	0.500	386.409	0.011	0.000	0.011	0.000	0.001	0.500	8451.755
		LR	0.523	0.523	0.523	0.523	0.520	0.520	469.512	0.001	0.000	0.001	0.000	0.001	0.500	1481.505
		DT	0.535	0.286	0.535	0.373	0.348	0.500	308.698	0.042	0.001	0.042	0.003	0.004	0.499	2764.815
	PWM2Vec [21]	NB	0.468	0.508	0.468	0.331	0.351	0.500	60.008	0.034	0.004	0.034	0.003	0.004	0.499	370.330
		MLP	0.471	0.503	0.471	0.369	0.385	0.500	333.503	0.400	0.335	0.400	0.355	0.080	0.534	577.936
		KNN	0.520	0.575	0.520	0.470	0.480	0.542	4565.427	0.061	0.213	0.061	0.089	0.059	0.496	2475.871
		RF	0.535	0.286	0.535	0.372	0.348	0.500	746.999	0.034	0.001	0.034	0.002	0.003	0.500	10880.182
		LR	0.534	0.603	0.534	0.482	0.492	0.557	975.877	0.001	0.012	0.001	0.009	0.009	0.490	278.851
		DT	0.535	0.286	0.535	0.372	0.348	0.500	500.541	0.022	0.001	0.022	0.032	0.013	0.500	3078.085
Minimizer	NB	0.523	0.529	0.523	0.523	0.523	0.526	65.955	0.062	0.194	0.062	0.048	0.055	0.525	497.483	
	MLP	0.477	0.495	0.477	0.447	0.455	0.494	499.569	0.005	0.003	0.005	0.003	0.008	0.475	707.236	
	KNN	0.539	0.538	0.539	0.538	0.535	0.536	5211.216	0.177	0.155	0.177	0.148	0.058	0.522	3116.525	
	RF	0.535	0.287	0.535	0.373	0.348	0.499	624.564	0.034	0.001	0.034	0.002	0.003	0.500	10349.430	
	LR	0.548	0.548	0.548	0.548	0.546	0.546	771.273	0.201	0.120	0.201	0.228	0.102	0.501	3234.386	
	DT	0.464	0.215	0.464	0.294	0.317	0.500	576.693	0.003	0.002	0.003	0.002	0.003	0.500	346.660	

original embedding data. We use 10% of the original counts to generate the synthetic embeddings respectively.

For Influenza A Virus data the results show that in some cases the addition of GANs-based synthetic data improves the performance as compared to the performance on the original data, like for the KNN, RF, and NB classifiers corresponding to PWM2Vec methods. Similarly, on the VDJDB dataset, the GAN-based improvement is also witnessed in some cases, like for all the classifiers corresponding to the PWM2Vec method except NB. Moreover, as the performance of the PALmdb dataset on the original data is maximum already, the addition of GAN embeddings has retained that maximum performance.

C. Performance of only GANs Data

We also studied the classification performance gain of using only GANs-based embeddings without the original data. The results depict that for all the 3 datasets, this category has the lowest predictive performance for all the combinations of classifiers and embeddings as compared to the performance on original data and on original data with GANs. As only the synthetic data is employed to train the classifiers, while they

are tested on the original data, which is why the performance is low as compared to others.

Generally, we can observe that the inclusion of GAN synthetic data in the training set can improve the overall classification performance. This is because the training set size is increased and its data imbalance issue is resolved by adding the respective synthetic data.

D. Statistical Significance

To determine the statistical significance of our classification results, we performed a student t-test and calculated the p -values using the average and standard deviation of five runs. Our analysis revealed that the majority of p -values were less than 0.05, and this was true for all embedding methods, as the standard deviation values were very low. These findings confirm the statistical significance of our results.

VI. CONCLUSION

In conclusion, this work explores a novel approach to improve the predictive performance of the biological sequence classification task by using GANs. It generates synthetic data

TABLE V: The antigen species-wise classification results of VDjDB dataset. These results are average values over 5 runs.

Method	Algo.	Acc. \uparrow	Prec. \uparrow	Recall \uparrow	F1 (Weig.) \uparrow	F1 (Macro) \uparrow	ROC AUC \uparrow	Train Time (Sec.) \downarrow	
Without GANs	Spike2Vec [20]	NB	0.999	0.999	0.999	0.999	0.999	0.999	87.948
		MLP	0.999	0.999	0.999	0.999	0.999	0.999	689.357
		KNN	0.998	0.998	0.998	0.998	0.998	0.999	167.426
		RF	0.999	0.999	0.999	0.999	0.999	0.999	152.581
		LR	0.999	0.999	0.999	0.999	0.999	0.999	882.695
	DT	0.999	0.999	0.999	0.999	0.999	0.999	43.314	
	PWM2Vec [21]	NB	0.179	0.926	0.179	0.250	0.305	0.634	84.292
		MLP	0.525	0.685	0.525	0.399	0.315	0.626	1216.913
		KNN	0.525	0.689	0.525	0.399	0.320	0.626	248.660
		RF	0.525	0.690	0.525	0.400	0.320	0.626	736.583
		LR	0.525	0.681	0.525	0.400	0.320	0.626	299.575
	DT	0.525	0.690	0.525	0.400	0.320	0.626	39.697	
	Minimizer	NB	0.930	0.972	0.930	0.940	0.838	0.935	98.159
		MLP	0.934	0.952	0.934	0.928	0.782	0.882	1253.018
		KNN	0.951	0.961	0.951	0.947	0.849	0.925	172.851
RF		0.953	0.962	0.953	0.948	0.847	0.927	468.139	
LR		0.952	0.961	0.952	0.948	0.847	0.926	203.061	
DT	0.952	0.962	0.952	0.948	0.847	0.926	25.392		
With GANs	Spike2Vec [20]	NB	0.999	0.999	0.999	0.999	0.988	0.999	78.891
		MLP	0.999	0.999	0.999	0.999	0.999	0.999	1085.850
		KNN	0.998	0.998	0.998	0.998	0.992	0.998	135.567
		RF	0.999	0.999	0.999	0.999	0.999	0.999	186.662
		LR	0.999	0.999	0.999	0.999	0.999	0.999	5736.169
	DT	0.999	0.999	0.999	0.999	0.999	0.999	143.618	
	PWM2Vec [21]	NB	0.151	0.926	0.151	0.247	0.234	0.603	109.493
		MLP	0.529	0.685	0.529	0.403	0.231	0.595	358.965
		KNN	0.531	0.689	0.531	0.406	0.317	0.625	126.428
		RF	0.532	0.691	0.532	0.408	0.319	0.625	1052.845
		LR	0.528	0.690	0.528	0.403	0.321	0.626	5643.762
	DT	0.528	0.691	0.528	0.403	0.321	0.626	142.579	
	Minimizer	NB	0.916	0.989	0.916	0.943	0.801	0.916	90.476
		MLP	0.952	0.961	0.952	0.948	0.851	0.927	440.944
		KNN	0.951	0.960	0.951	0.947	0.844	0.926	149.858
RF		0.953	0.961	0.953	0.949	0.850	0.927	527.874	
LR		0.952	0.961	0.952	0.948	0.849	0.927	4918.374	
DT	0.952	0.961	0.952	0.948	0.850	0.927	111.393		
Spike2Vec [20]	NB	0.002	0.000	0.002	0.000	0.001	0.491	98.736	
	MLP	0.022	0.139	0.022	0.032	0.019	0.479	222.333	
	KNN	0.106	0.139	0.106	0.076	0.123	0.558	368.164	
	RF	0.010	0.000	0.010	0.000	0.001	0.500	665.565	
	LR	0.200	0.136	0.200	0.091	0.020	0.500	3497.008	
DT	0.190	0.036	0.190	0.061	0.018	0.499	467.308		
PWM2Vec [21]	NB	0.026	0.068	0.026	0.003	0.003	0.499	93.458	
	MLP	0.392	0.389	0.392	0.295	0.056	0.499	250.162	
	KNN	0.140	0.205	0.140	0.040	0.016	0.500	343.585	
	RF	0.477	0.227	0.477	0.308	0.038	0.500	644.587	
	LR	0.012	2.070	0.012	4.020	0.001	0.500	4498.689	
DT	0.002	4.170	0.002	8.324	0.000	0.500	498.689		
Minimizer	NB	0.023	0.215	0.023	0.035	0.033	0.510	115.915	
	MLP	0.420	0.597	0.420	0.448	0.081	0.514	274.471	
	KNN	0.551	0.690	0.551	0.600	0.152	0.599	382.306	
	RF	0.010	0.000	0.010	0.000	0.001	0.500	792.106	
	LR	0.514	0.235	0.514	0.385	0.047	0.500	3465.703	
DT	0.474	0.225	0.474	0.305	0.037	0.500	445.797		

with the help of GANs to eliminate the data imbalance challenge, hence improving the performance. In the future, we would like to extend this study by investigating more advanced variations of GANs to synthesize the biological sequences and their impacts on the biological sequence analysis. We also want to examine additional genetic data, such as hemagglutinin and neuraminidase gene sequences, with GANs to improve their classification accuracy.

REFERENCES

- [1] K. Das, "Antivirals targeting influenza a virus," *Journal of medicinal chemistry*, vol. 55, no. 14, pp. 6263–6277, 2012.
- [2] S. F. Pedersen, Y.-C. Ho *et al.*, "Sars-cov-2: a storm is raging," *The Journal of clinical investigation*, vol. 130, no. 5, pp. 2202–2205, 2020.
- [3] D. Rognan, "Chemogenomic approaches to rational drug design," *British journal of pharmacology*, vol. 152, no. 1, pp. 38–52, 2007.
- [4] G. Dong and J. Pei, *Sequence data mining*. Springer Science & Business Media, 2007, vol. 33.
- [5] A. Babaian and R. Edgar, "Ribovirus classification by a polymerase barcode sequence," *PeerJ*, vol. 10, p. e14055, 2022.
- [6] J. Hadfield, C. Megill, S. Bell, J. Huddleston, B. Potter, C. Callender, P. Sagulenko, T. Bedford, and R. Neher, "Nextstrain: real-time tracking of pathogen evolution," *Bioinformatics*, vol. 34, pp. 4121–4123, 2018.
- [7] B. Q. Minh *et al.*, "Iq-tree 2: New models and efficient methods for phylogenetic inference in the genomic era," *Molecular Biology and Evolution*, vol. 37, no. 5, pp. 1530–1534, 2020.
- [8] D. Chen, S. Li, and Y. Chen, "Istrf: Identification of sucrose transporter using random forest," *Frontiers in Genetics*, vol. 13, 2022.
- [9] L. Yang, Y.-H. Zhang, F. Huang, Z. Li, T. Huang, and Y.-D. Cai, "Identification of protein–protein interaction associated functions based on gene ontology and kegg pathway," *Frontiers in Genetics*, vol. 13, 2022.

- [10] X. Zhang, S. Wang, L. Xie, and Y. Zhu, "Pseu-st: A new stacked ensemble-learning method for identifying rna pseudouridine sites," *Frontiers in Genetics*, vol. 14, 2023.
- [11] K. Kuzmin *et al.*, "Machine learning methods accurately predict host specificity of coronaviruses based on spike sequences alone," *Biochemical and Biophysical Research Communications*, vol. 533, no. 3, pp. 553–558, 2020.
- [12] Y. Ma, Z. Yu, R. Tang, X. Xie, G. Han, and V. V. Anh, "Phylogenetic analysis of hiv-1 genomes based on the position-weighted k-mers method," *Entropy*, vol. 22, no. 2, p. 255, 2020.
- [13] M. Ghandi, D. Lee, M. Mohammad-Noori, and M. A. Beer, "Enhanced regulatory sequence prediction using gapped k-mer features," *PLoS computational biology*, vol. 10, no. 7, p. e1003711, 2014.
- [14] J. Shen, Y. Qu, W. Zhang, and Y. Yu, "Wasserstein distance guided representation learning for domain adaptation," in *AAAI conference on artificial intelligence*, 2018.
- [15] J. Xie, R. Girshick, and A. Farhadi, "Unsupervised deep embedding for clustering analysis," in *International conference on machine learning*, 2016, pp. 478–487.
- [16] M. Heinzinger, A. Elnaggar, Y. Wang, C. Dallago, D. Nechaev, F. Matthes, and B. Rost, "Modeling aspects of the language of life through transfer-learning protein sequences," *BMC bioinformatics*, vol. 20, no. 1, pp. 1–17, 2019.
- [17] N. Strodthoff, P. Wagner, M. Wenzel, and W. Samek, "Udmsprot: universal deep sequence models for protein classification," *Bioinformatics*, vol. 36, no. 8, pp. 2401–2409, 2020.
- [18] Y. Zhang, S. Qiao, R. Lu, N. Han, D. Liu, and J. Zhou, "How to balance the bioinformatics data: pseudo-negative sampling," *BMC bioinformatics*, vol. 20, no. 25, pp. 1–13, 2019.
- [19] S. M. Abd Elrahman and A. Abraham, "A review of class imbalance problem," *Journal of Network and Innovative Computing*, vol. 1, no. 2013, pp. 332–340, 2013.
- [20] S. Ali and M. Patterson, "Spike2vec: An efficient and scalable embedding approach for covid-19 spike sequences," in *IEEE International Conference on Big Data (Big Data)*, 2021, pp. 1533–1540.
- [21] S. Ali, B. Bello, P. Chourasia, R. T. Punathil, Y. Zhou, and M. Patterson, "Pwm2vec: An efficient embedding approach for viral host specification from coronavirus spike sequences," *MDPI Biology*, 2022.
- [22] H. Han, W.-Y. Wang, and B.-H. Mao, "Borderline-smote: a new over-sampling method in imbalanced data sets learning," in *Advances in Intelligent Computing: International Conference on Intelligent Computing, ICIC 2005, Hefei, China, August 23-26, 2005, Proceedings, Part I 1*. Springer, 2005, pp. 878–887.
- [23] X. Xiaolong, C. Wen, and S. Yanfei, "Over-sampling algorithm for imbalanced data classification," *Journal of Systems Engineering and Electronics*, vol. 30, no. 6, pp. 1182–1191, 2019.
- [24] X.-M. Zhao, X. Li, L. Chen, and A. Aihara, "Protein classification with imbalanced data," *Proteins: Structure, function, and bioinformatics*, vol. 70, no. 4, pp. 1125–1132, 2008.
- [25] B. Tang and H. He, "Kerneladasy: Kernel based adaptive synthetic data generation for imbalanced learning," in *2015 IEEE congress on evolutionary computation (CEC)*. IEEE, 2015, pp. 664–671.
- [26] G. Douzas and F. Bacao, "Effective data generation for imbalanced learning using conditional generative adversarial networks," *Expert Systems with applications*, vol. 91, pp. 464–471, 2018.
- [27] M. Roberts, W. Haynes, B. Hunt, S. Mount, and J. Yorke, "Reducing storage requirements for biological sequence comparison," *Bioinformatics*, vol. 20, pp. 3363–9, 2004.
- [28] Bacterial and Viral Bioinformatics Resource Center, <https://www.bv-brc.org/>.
- [29] R. C. Edgar, J. Taylor, V. Lin, T. Altman, P. Barbera, D. Meleshko, D. Lohr, G. Novakovskiy, B. Buchfink, B. Al-Shayeb *et al.*, "Petabase-scale sequence alignment catalyses viral discovery," *Nature*, vol. 602, no. 7895, pp. 142–147, 2022.
- [30] D. V. Bagaev, R. M. Vroomans, J. Samir, U. Stervbo, C. Rius, G. Dolton, A. Greenshields-Watson, M. Attaf, E. S. Egorov, I. V. Zvyagin *et al.*, "Vdjdbs in 2019: database extension, new analysis infrastructure and a t-cell receptor motif compendium," *Nucleic Acids Research*, vol. 48, no. D1, pp. D1057–D1062, 2020.
- [31] L. Van der M. and G. Hinton, "Visualizing data using t-sne," *Journal of Machine Learning Research (JMLR)*, vol. 9, no. 11, 2008.